

STRATEGIC CLASSIFICATION WITH GRAPH NEURAL NETWORKS

Itay Eilat *

Department of Computer Science
Technion
Haifa, Israel
itayeilat@campus.technion.ac.il

Ben Finkelstein *

Department of Computer Science
Technion
Haifa, Israel
benfin@campus.technion.ac.il

Chaim Baskin

Department of Computer Science
Technion
Haifa, Israel
chaimbaskin@technion.ac.il

Nir Rosenfeld

Department of Computer Science
Technion
Haifa, Israel
nirr@technion.ac.il

ABSTRACT

Strategic classification studies learning in settings where users can modify their features to obtain favorable predictions. Most current works focus on simple classifiers that trigger independent user responses. Here we examine the implications of learning with more elaborate models that break the independence assumption. Motivated by the idea that applications of strategic classification are often social in nature, we focus on *graph neural networks*, which make use of social relations between users to improve predictions. Using a graph for learning introduces inter-user dependencies in prediction; our key point is that strategic users can exploit these to promote their own goals. As we show through analysis and simulation, this can work either against the system—or for it. Based on this, we propose a differentiable framework for strategically-robust learning of graph-based classifiers. Experiments on several real networked datasets demonstrate the utility of our approach.

1 INTRODUCTION

Machine learning is increasingly being used to inform decisions about humans. But when users of a system stand to gain from certain predictive outcomes, they may be prone to “game” the system by strategically modifying their features (at some cost). The literature on *strategic classification* (Brückner & Scheffer, 2011; Hardt et al., 2016) studies learning in this setting, with emphasis on how to learn classifiers that are robust to strategic user behavior. The idea that users may respond to a decision rule applies broadly and across many domains, from hiring, admissions, and scholarships, to loan approval, insurance, welfare benefits, and medical eligibility (McCrory, 2008; Almond et al., 2010; Camacho & Conover, 2011; Lee & Lemieux, 2010). This, along with its clean formulation as a learning problem, have made strategic classification the target of much recent interest (Sundaram et al., 2021; Zhang & Conitzer, 2021; Levanon & Rosenfeld, 2021; Ghalme et al., 2021; Jagadeesan et al., 2021; Zrnic et al., 2021; Estornell et al., 2021; Lechner & Urner, 2021; Harris et al., 2021; Levanon & Rosenfeld, 2022; Liu et al., 2022; Ahmadi et al., 2022; Barsotti et al., 2022a).

But despite these advances, most works in strategic classification remain to follow the original problem formulation in assuming independence across users responses. From a technical perspective, this assumption greatly simplifies the learning task, as it allows the classifier to consider each user’s response in isolation: user behavior is modeled via a *response mapping* $\Delta_h(x)$ determining how users modify their features x in response to the classifier h , and learning aims to find an h for which $y \approx h(\Delta_h(x))$. Intuitively, a user will modify her features if this ‘moves’ her across the decision boundary, as long as this is worthwhile (i.e., gains from prediction exceed modification costs). Knowing Δ_h allows the system to anticipate user responses and learn an h that is robust.

¹Equal contribution, alphabetical order

For a wide range of settings, learning under independent user responses has been shown to be theoretically possible (Hardt et al., 2016; Zhang & Conitzer, 2021; Sundaram et al., 2021) and practically feasible (Levanon & Rosenfeld, 2021; 2022). Unfortunately, once this assumption of independence is removed—results no longer hold. One reason is that current approaches can safely assume independence because the decision rules they consider *induce* independence: when predictions inform decisions for each user independently, users have no incentive to account for the behavior of others. This limits the scope of predictive models to include only simple functions of single inputs.

In this paper, we aim to extend the literature on strategic classification to support richer learning paradigms that enable inter-dependent user responses, with particular focus on the domain of Graph Neural Networks (GNNs) (Monti et al., 2017; Wang et al., 2019; Bronstein et al., 2017; Hamilton et al., 2017). Generally, user responses can become dependent through the classifier if predictions for one user rely also on information regarding other users, i.e., if $h(x_i)$ is also a function of other x_j . In this way, the affects of a user modifying her features via $x_j \mapsto \Delta_h(x_j)$ can propagate to other users and affect their decisions (since $h(x_i)$ now relies on $\Delta_h(x_j)$ rather than x_j). For GNNs, this expresses through their reliance on the graph. GNNs take as input a weighted graph whose nodes correspond to featurized examples, and whose edges indicate relations that are believed to be useful for prediction (e.g., if $j \rightarrow i$ indicates that $y_i = y_j$ is likely). In our case, nodes represent users, and edges represent social links. The conventional approach is to first embed nodes in a way that depends on their neighbors' features, $\phi_i = \phi(x_i; x_{\text{nei}(i)})$, and then perform classification (typically linear) in embedded space, $\hat{y}_i = \text{sign}(w^\top \phi_i)$. Notice \hat{y}_i depends on x_i , but also on all other $x_j \in x_{\text{nei}(i)}$; hence, in deciding how to respond, user i must also account for the strategic responses of her neighbors $j \in \text{nei}(i)$. We aim to establish the affects of such dependencies on learning.

As a concrete example, consider Lenddo¹, a company that provides credit scoring services to lending institutions. Lenddo specializes in consumer-focused microlending for emerging economies, where many applicants lack credible financial records. To circumvent the need to rely on historical records, Lenddo uses applicants' social connections, which are easier to obtain, as a factor in their scoring system.² As an algorithmic approach for this task, GNNs are an adequate choice (Gao et al., 2021). Once loan decisions become dependent on social relations, the incentives for acting strategically change (Wei et al., 2016). To see how, consider that a user who lies far to the negative side of the decision boundary (and so independently cannot cross) may benefit from the graph if her neighbors “pull” her embedding towards the decision boundary and close enough for her to cross. Conversely, the graph can also suppress strategic behavior, since neighbors can “hold back” nodes and prevent them from crossing. Whether this is helpful to the system or not depends on the true label of the node.

This presents a tradeoff: In general, graphs are useful if they are informative of labels in a way that complements features; the many success stories of GNNs suggest that this is often the case (Zhou et al., 2020). But even if this holds *sans* strategic behavior—once introduced, graphs inadvertently create dependencies through user representations, which strategic users can exploit. Graphs therefore hold the potential to benefit the system, but also its users. Here we study the natural question: who does the graph help more? Through analysis and experimentation, we show that learning in a way that *neglects* to account for strategic behavior not only jeopardizes performance, but becomes *worse* as reliance on the graph increases. In this sense, the graph becomes a vulnerability which users can utilize for their needs, turning it from an asset to the system—to a potential threat.

As a solution, we propose a practical approach to learning GNNs in strategic environments. We show that for a key neural architecture (SGC; Wu et al. (2019)) and certain cost functions, graph-dependent user responses can be expressed as a ‘projection-like’ operator. This operator admits a simple and differentiable closed form; with additional smoothing, this allows us to implement responses as a neural layer, and learn robust predictors h using gradient methods. Experiments on synthetic and real data (with simulated responses) demonstrate that our approach not only effectively accounts for strategic behavior, but in some cases, can harness the efforts of self-interested users to promote the system’s goals. Our code is anonymously available at: <http://github.com/StrategicGNNs/Code>.

¹<http://lenddoefl.com>; see also <http://www.wired.com/2014/05/lenddo-facebook/>.

²For a discussion on ethics, see final section. For similar initiatives, see <https://en.wikipedia.org/wiki/Lenddo>.

1.1 RELATED WORK

Strategic classification. Since its introduction in Hardt et al. (2016) (and based on earlier formulations in Brückner & Scheffer (2009); Brückner et al. (2012); Großhans et al. (2013)), the literature on strategic classification has been growing at a rapid pace. Various aspects of learning have been studied, including: generalization behavior (Zhang & Conitzer, 2021; Sundaram et al., 2021; Ghalme et al., 2021), algorithmic hardness (Hardt et al., 2016), practical optimization methods (Levanon & Rosenfeld, 2021; 2022), and societal implications (Milli et al., 2019; Hu et al., 2019; Chen et al., 2020; Levanon & Rosenfeld, 2021). Some efforts have been made to extend beyond the conventional user models, e.g., by adding noise (Jagadeesan et al., 2021), relying on partial information Ghalme et al. (2021); Bechavod et al. (2022), or considering broader user interests Levanon & Rosenfeld (2022); but these, as do the vast majority of other works, focus on linear classifiers and independent user responses.³ We study richer predictive model classes that lead to correlated user behavior.

Graph Neural Networks (GNNs). The use of graphs in learning has a long and rich history, and remains a highly active area of research (Wu et al., 2020). Here we cover a small subset of relevant work. The key idea underlying most methods is to iteratively propagate and aggregate information from neighboring nodes. Modern approaches implement variations of this idea as differentiable neural architectures (Gori et al., 2005; Scarselli et al., 2008; Kipf & Welling, 2017; Gilmer et al., 2017). This allows to express more elaborate forms of propagation (Li et al., 2018; Alon & Yahav, 2021) and aggregation (Wu et al., 2019; Xu et al., 2019; Li et al., 2016), including attention-based mechanisms (Veličković et al., 2018; Brody et al., 2022). Nonetheless, a key result by Wu et al. (2019) shows that, both theoretically and empirically, linear GNNs are also quite expressive.

Robustness of GNNs. As most other fields in deep learning, GNNs have been the target of recent inquiry as to their sensitivity to adversarial attacks. Common attacks include perturbing nodes, either in sets (Zügner et al., 2018; Zang et al., 2021) or individually (Finkelshtein et al., 2020). Attacks can be applied before training (Zügner & Günnemann, 2019; Bojchevski & Günnemann, 2019; Li et al., 2021; Zhang & Zitnik, 2020) or at test-time (Szegedy et al., 2014; Goodfellow et al., 2015); our work corresponds to the latter. While there are connections between adversarial and strategic behavior (Sundaram et al., 2021), the key difference is that strategic behavior is not a zero-sum game; in some cases, incentives can even align (Levanon & Rosenfeld, 2022). Thus, system-user relations become more nuanced, and provide a degree of freedom in learning that does not exist in adversarial settings.

2 LEARNING SETUP

Our setting includes n users, represented as nodes in a directed graph $G = (V, E)$ with non-negative edge weights $W = \{w_{ij}\}_{(i,j) \in E}$, $w_{ij} \geq 0$. Each user i is also described by a feature vector $x_i \in \mathbb{R}^\ell$ and a binary label $y_i \in \{\pm 1\}$. We use $x_{-i} = \{x_j\}_{j \neq i}$ to denote the set of features of all nodes other than i . Using the graph, our goal is to learn a classifier h that correctly predicts user labels. The challenge in our strategic setting is that inputs at test-time can be strategically modified by users, in response to h and in a way that depends on the graph and on other users (we describe this shortly). Denoting by x_i^h the (possibly modified) strategic response of i to h , our learning objective is:

$$\operatorname{argmin}_{h \in H} \sum_i L(y_i, \hat{y}_i), \quad \hat{y}_i = h(x_i^h; x_{-i}^h) \quad (1)$$

where H is the model class and L is a loss function (i.e., log-loss). Note that both predictions \hat{y}_i and modified features x_i^h can depend on G and on on x_{-i}^h (possibly indirectly through h). We focus on the inductive graph learning setting, in which training is done on G , but testing is done on a different graph, G' (often G, G' are two disjoint components of a larger graph). Our goal is therefore to learn a classifier that generalizes to other graphs in a way that is robust to strategic user behavior.

Graph-based learning. We consider linear graph-based classifiers—these are linear classifiers that operate on linear, graph-dependent node embeddings, defined as:

$$h_{\theta,b}(x_i; x_{-i}) = \operatorname{sign}(\theta^\top \phi(x_i; x_{-i}) + b), \quad \phi(x_i; x_{-i}) = \tilde{w}_{ii}x_i + \sum_{j \neq i} \tilde{w}_{ji}x_j \quad (2)$$

³The only exception we know of is Liu et al. (2022) who study strategic ranking, but do not consider learning.

where $\phi_i = \phi(x_i; x_{-i})$ is node i 's embedding,⁴ $\theta \in \mathbb{R}^\ell$ and $b \in \mathbb{R}$ are learned parameters, and $\tilde{w}_{ij} \geq 0$ are pairwise weights that depend on G and W . We refer to users j with $\tilde{w}_{ji} \neq 0$ as the *embedding neighbors* of i . A simple choice of weights is $\tilde{w}_{ji} = w_{ji}$ for $(j, i) \in E$ (and 0 otherwise), but different methods propose different ways to construct \tilde{w} ; here we adopt the weight scheme of Wu et al. (2019). We assume the weights \tilde{w} are predetermined, and aim to learn θ and b in Eq. (1).

Our focus on linear GNNs stems from several factors. From the perspective of strategic classification, linear decision rules ensure that strategic responses are computationally tractable (see Eq. (4)). This is conventionally required, and most works remain in the linear regime. From the perspective of GNNs, linear architectures have been shown to match state-of-the-art performance on multiple tasks (Wu et al., 2019), implying sufficiently manifest the fundamental role of graphs. Thus, linear GNNs serve as a minimal necessary step for bridging standard strategic classification and graph-based learning, in a way that captures the fundamental structure of the learning task in both domains. Nonetheless, as we show in Sec. 4, even for linear GNNs—user responses can cause learning to be highly non-linear.

Strategic inputs. For the strategic aspects of our setting, we build on the popular formulation of Hardt et al. (2016). Users seek to be classified positively (i.e., have $\hat{y}_i = 1$), and to achieve this, are willing to modify their features (at some cost). Once the system has learned and published h , a test-time user i can modify her features $x_i \mapsto x'_i$ in response to h . Modification costs are defined by a cost function $c(x, x')$ (known to all); here we focus mainly on 2-norm costs $c(x, x') = \|x - x'\|_2$ (Levanon & Rosenfeld, 2022; Chen et al., 2020), but also discuss other costs (Brückner et al., 2012; Levanon & Rosenfeld, 2021; Bechavod et al., 2022). User i modifies her features (or “moves”) if this improves her prediction (i.e., if $h(x_i) = -1$ but $h(x'_i) = 1$) and is cost-effective (i.e., prediction gains exceed modification costs); for linear classifiers, this means crossing the decision boundary. Note that since $y \in \{\pm 1\}$, gains are at most $h(x') - h(x) = 2$. Users therefore do not move to any x' whose cost $c(x, x')$ exceeds a ‘budget’ of 2, and the maximal moving distance is $d = 2$.

Distribution shift. One interpretation of strategic classification is that user responses cause *distribution shift*, since in aggregate, $p(x') \neq p(x)$. Crucially, *how* the distribution changes depends on h , which implies that the system has some control over the test distribution $p(x')$, indirectly through user how users respond—a special case of model-induced distribution shift (Miller et al., 2021; Maheshwari et al., 2022). The unique aspect of our setting is that user responses are linked through their mutual dependence on the graph. We next describe our model of user responses in detail.

3 STRATEGIC USER BEHAVIOR: MODEL AND ANALYSIS

Eq. (2) states that h classifies i according to her embedding ϕ_i , which in turn is a weighted sum of her features and those of her neighbors. To gain intuition as to the effects of the graph on user behavior, it will be convenient to assume weights \tilde{w} are normalized⁵ so that we can write:

$$\phi_i = \phi(x_i; x_{-i}) = (1 - \alpha_i)x_i + \alpha_i\bar{x}_i \quad \text{for some } \alpha_i \in [0, 1] \quad (3)$$

I.e., ϕ_i can be viewed as an interpolation between x_i and some point $\bar{x}_i \in \mathbb{R}^\ell$ representing all other nodes, where the precise point along the line depends on a parameter α_i that represents the influence of the graph (in a graph-free setting, $\alpha_i = 0$). This reveals the dual effect a graph has on users: On the one hand, the graph limits the ability of user i to influence her own embedding, since any effort invested in modifying x_i affects ϕ_i by at most $1 - \alpha_i$. But the flip side of this is that an α_i -portion of ϕ_i is fully determined by other users (as expressed in \bar{x}_i); if they move, i 's embedding also ‘moves’ for free. A user's ‘effective’ movement radius is $r_i = d(1 - \alpha_i)$. Fig. 1 (F) shows this for varying α_i .

3.1 STRATEGIC RESPONSES

Given that h relies on the graph for predictions—how should a user modify her features x_i to obtain $\hat{y}_i = 1$? In vanilla strategic classification (where h operates on each x_i independently), users are modeled as rational agents that respond to the classifier by maximizing their utility, i.e., play $x'_i = \text{argmax}_{x_i} h(x') - c(x_i, x')$, which is a best-response that results in immediate equilibrium

⁴Note that embedding preserve the dimension of the original features.

⁵This is indeed the case in several common approaches.

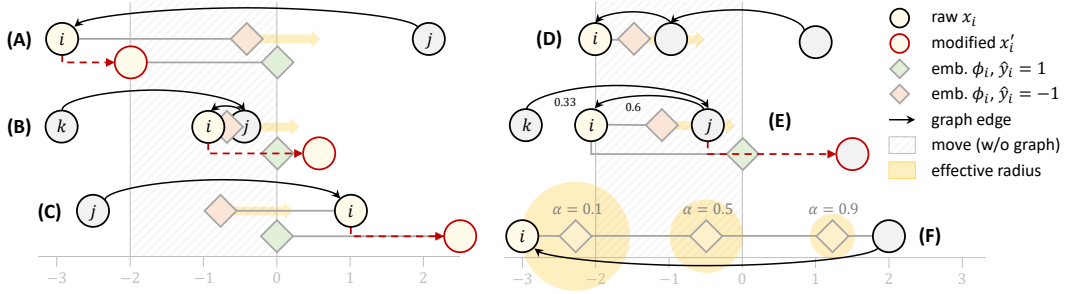


Figure 1: **Simple graphs, complex behavior.** In all examples h_b has $b = 0$, and $\tilde{w}_{ij} = 1$ unless otherwise noted. (A) Without the graph, i does not move, but with $j \rightarrow i$, ϕ_i is close enough to cross. (B) i can cross, but due to $j \rightarrow i$, must move beyond 0. (C) Without the graph, i has $\hat{y}_i = 1$, but due to $j \rightarrow i$, must move. (D) Without the graph i would move, but with the graph—cannot. (E) Hitchhiker: i cannot move, but once j moves and crosses, ϕ_i crosses for free. (F) Effective radii for various α .

(users have no incentive to move, and the system has no incentive to change h).⁶ In our graph-based setting, however, the dependence of \hat{y}_i on all other users via $h(x_i; x_{-i})$ makes this notion of best-response ill-defined, since the optimal x'_i can depend on others' strategic responses, x'_{-i} , which are unknown to user i at the time of decision (and may very well rely on x'_i itself).

As a feasible alternative, here we generalize the standard model by assuming that users play *myopic best-response* over a sequence of multiple update rounds. As we will see, this has direct connections to key ideas underlying graph neural networks. Denote the features of node i at round t by $x_i^{(t)}$, and set $x_i^{(0)} = x_i$. A myopic best response means that at round t , each user i chooses $x_i^{(t)}$ to maximize her utility at time t according to the state of the game at time $t-1$, i.e., assuming all other users play $\{x_j^{(t-1)}\}_{j \neq i}$, with costs accumulating over rounds. This defines a *myopic response mapping*:

$$\Delta_h(x_i; x_{-i}, \kappa) \triangleq \underset{x' \in \mathbb{R}^{\ell}}{\operatorname{argmax}} h(x'; x_{-i}) - c(x_i, x') - \kappa \quad (4)$$

where at round t updates are made (concurrently) via $x_i^{(t+1)} = \Delta_h(x_i^{(t)}; x_{-i}^{(t)}, \kappa_i^{(t)})$ with accumulating costs $\kappa_i^{(t)} = \kappa_i^{(t-1)} + c(x_i^{(t-1)}, x_i^{(t)})$, $\kappa_i^{(0)} = 0$. Predictions for round t are $\hat{y}_i^{(t)} = h(x_i^{(t)}; x_{-i}^{(t)})$.

Eq. (4) naturally extends the standard best-response mapping (which is recovered when $\alpha_i = 0 \forall i$, and converges after one round). By adding a temporal dimension, the actions of users propagate over the graph and in time to affect others. Nonetheless, even within a single round, graph-induced dependencies can result in non-trivial behavior; some examples for $\ell = 1$ are given in Fig. 1 (A-D).

3.2 ANALYSIS

We now give several results demonstrating basic properties of our response model and consequent dynamics, which shed light on how the graph differentially affects the system and its users.

Convergence. Although users are free to move at will, movement adheres to a certain useful pattern.

Proposition 1. For any h , if users move via Eq. (4), then for all $i \in [n]$, $x_i^{(t)} \neq x_i^{(t-1)}$ at most once.

Proof. User i will move only when: (i) she is currently classified negatively, $h(x_i; x_{-i}) = -1$, and (ii) there is some x' for which utility can improve, i.e., $h(x'; x_{-i}) - c(x_i, x') > -1$, which in our case occurs if $h(x'; x_{-i}) = 1$ and $c(x_i, x') < 2$ (since h maps to $[-1, 1]$).⁷ Eq. (4) ensures that the

⁶Note ‘rational’ here implies users are assumed to know h . As most works in the field, we also make this assumption; for the practically-inclined reader, note that (i) in some cases, there is reason to believe it may approximately hold (e.g., <http://openschufa.de>), and (ii) relaxing this assumption (and others) is an ongoing community effort (Ghalme et al., 2021; Jagadeesan et al., 2021; Bechavod et al., 2022; Barsotti et al., 2022b).

⁷In line with Hardt et al. (2016), we assume that if the value is zero then the user does not move.

modified x'_i will be such that $\phi(x'_i; x_{-i})$ lies exactly on the decision boundary of h ; hence, x'_i must be *closer* to the decision boundary (in Euclidian distance) than x_i . This means that any future moves of an (incoming) neighbor j can only push i further away from the decision boundary; hence, the prediction for i remains positive, and she has no future incentive to move again.⁸ \square

Hence, all users move at most once. The proof reveals a certain monotonicity principle: users always (weakly) benefit from any strategic movement. Convergence follows as an immediate result.

Corollary 1. *Myopic-best response dynamics converge for any h (and after at most n rounds).*

We will henceforth use x_i^h to denote the features of user i at convergence (w.r.t. h), denoted T_{\max} .

Hitchhiking. When i moves, the embeddings of (outgoing) neighbors j who currently have $\hat{y}_j = -1$ also move closer to the decision boundary; thus, users who were initially too far to cross may be able to do so at later rounds. In this sense, the dependencies across users introduced by the graph-dependent embeddings align user incentives, and promote an implicit form of cooperation. Interestingly, users can also obtain positive predictions *without* moving. We refer to such users as ‘hitchhikers’.

Proposition 2. *There exist cases where $\hat{y}_i^{(t)} = -1$ and i doesn’t move, but $\hat{y}_i^{(t+1)} = 1$.*

A simple example can be found in Figure 1 (E). Hitchhiking demonstrates how relying on the graph for classification can promote strategic behavior—even under a single response round.

Cascading behavior. Hitchhiking shows how the movement of one user can flip the label of another, but the effects of this process are constrained to a single round. When considering multiple rounds, a single node can trigger a ‘domino effect’ of moves that span the entire sequence.

Proposition 3. *For any n , there exists a graph where a single move triggers n additional rounds.*

Proposition 4. *For any n and $k \leq n$, there exists a graph where $n - k$ users move at round k .*

Proofs are constructive and modular (see Appendix A.2), so that increasing n can be done by attaching additional components. Both results show that, through monotonicity, users also (weakly) benefit from additional rounds. This has concrete implications on learning.

Corollary 2. *In the worst case, the number of rounds until convergence is $\Omega(n)$.*

Corollary 3. *In the worst case, $\Omega(n)$ users move after $\Omega(n)$ rounds.*

Thus, to exactly account for user behavior, the system must correctly anticipate the strategic responses of users many rounds into the future, since a bulk of predictions may flip in the last round. Fortunately, these results also suggests that in some cases, blocking one node from crossing can prevent a cascade of flips; thus, it may be worthwhile to ‘sacrifice’ certain predictions for collateral gains. This presents an interesting tradeoff in learning, encoded in the learning objective we present next.

4 LEARNING AND OPTIMIZATION

We are now ready to describe our learning approach. Our learning objective can be restated as:

$$\hat{h} = \operatorname{argmin}_{h \in H} \sum_i L(y_i, h(x_i^h; x_{-i}^h)) \quad (5)$$

for $H = \{h_{\theta, b}\}$ as in Eq. (2). The difficulty in optimizing Eq. (5) is that x^h depend on h through the iterative process, which relies on Δ_h . At test time, x^h can be computed exactly by simulating the dynamics. However, at train time, we would like to allow for gradients of θ, b to propagate through x^h . For this, we propose an efficient differential proxy of x^h , implemented as a stack of layers, each corresponding to one response round. The number of layers is a hyperparameter, T .

⁸Users moving only once ensures that cumulative costs are never larger than the final gain.

Single round. We begin with examining a single iteration of the dynamics, i.e., $T = 1$. Note that since a user moves only if the cost is at most 2, Eq. (4) can be rewritten as:

$$\Delta_h(x_i; x_{-i}) = \begin{cases} x'_i & \text{if } h(x_i; x_{-i}) = -1 \text{ and } c(x_i, x'_i) \leq 2 \\ x_i & \text{o.w.} \end{cases} \quad (6)$$

where $x'_i = \text{proj}_h(x_i; x_{-i})$ is the point to which x_i must move in order for $\phi(x_i; x_{-i})$ to be projected onto h . This projection-like operator (on x_i) can be shown to have a closed-form solution:

$$\text{proj}_h(x_i; x_{-i}) = x_i - \frac{\theta^\top \phi(x_i; x_{-i}) + b}{\|\theta\|_2^2 \tilde{w}_{ii}} \theta \quad (7)$$

See Appendix B.1 for a derivation using KKT conditions. Eq. (7) is differentiable in θ and b ; to make the entire response mapping differentiable, we replace the ‘hard if’ in Eq. (6) with a ‘soft if’, which we now describe. First, to account only for negatively-classified points, we ensure that only points in the negative halfspace are projected via a ‘positive-only’ projection:

$$\text{proj}_h^+(x_i; x_{-i}) = x_i - \min \left\{ 0, \frac{\theta^\top \phi(x_i; x_{-i}) + b}{\|\theta\|_2^2 \tilde{w}_{ii}} \right\} \theta \quad (8)$$

Then, we replace the $c \leq 2$ constraint with a smoothed sigmoid that interpolates between x_i and the projection, as a function of the cost of the projection and thresholded at 2. This gives our differentiable approximation of the response mapping:

$$\tilde{\Delta}(x_i; x_{-i}, \kappa) = x_i + (x'_i - x_i) \sigma_\tau(2 - c(x_i, x'_i) - \kappa) \quad \text{where } x'_i = \text{proj}_h^+(x_i; x_{-i}) \quad (9)$$

where σ is a sigmoid and τ is a temperature hyperparameter ($\tau \rightarrow 0$ recovers Eq. (6)) and for $T = 1$, $\kappa = 0$. In practice we add a small additive tolerance term for numerical stability (See Appendix B.3).

Multiple rounds. Next, we consider the computation of (approximate) modified features after $T > 1$ rounds, denoted $\tilde{x}^{(T)}$, in a differentiable manner. Our approach is to apply $\tilde{\Delta}$ iteratively as:

$$\tilde{x}_i^{(t+1)} = \tilde{\Delta}(\tilde{x}_i^{(t)}; \tilde{x}_{-i}^{(t)}, \kappa_i^{(t)}), \quad \tilde{x}_i^{(0)} = x_i \quad (10)$$

Considering $\tilde{\Delta}$ as a layer in a neural network, approximating T rounds can be done by stacking.

In Eq. (10), $\kappa_i^{(t)}$ is set to accumulate costs of approximate responses, $\kappa_i^{(t)} = \kappa_i^{(t-1)} + c(\tilde{x}_i^{(t-1)}, \tilde{x}_i^{(t)})$. One observation is that for 2-norm costs, $\kappa_i^{(t)} = c(\tilde{x}_i^{(0)}, \tilde{x}_i^{(t)})$ (by the triangle inequality; since all points move along a line, equality holds). We can therefore simplify Eq. (9) and replace $c(x_i^{(t-1)}, x'_i) - \kappa_i^{(t-1)}$ with $c(x_i^{(0)}, x'_i)$. For other costs, this gives a lower bound (see Appendix B.1).

5 EXPERIMENTS

5.1 SYNTHETIC DATA

We begin our empirical evaluation by demonstrating different aspects of learning in our setting using a simple but illustrative synthetic example. We set $\ell = 1$ and sample features $x_i \in \mathbb{R}$ for each class from a corresponding Gaussian $\mathcal{N}(y, 1)$ (classes are balanced). For each node we uniformly sample 5 neighbors from the same class and 3 from the other, and use uniform weights. This creates a task where both features and the graph are informative about labels, but only partially, and in a complementary manner (i.e., noise is uncorrelated; for i with $y_i = 1$, if $x_i < 0$, it is still more likely that most neighbors have $x_j > 0$, and vice versa). As it is a-priori unclear how to optimally combine these sources, we study the effects of relying on the graph to various degrees by varying a global α , i.e., setting $\tilde{w}_{ii} = (1 - \alpha)$ and $\tilde{w}_{ij} = \alpha/\deg_i$ for all i and all $j \neq i$. We examine both strategic and non-strategic settings, the latter serving as a benchmark. Since $\ell = 1$, $H = \{h_b\}$ is simply the class of thresholds, hence we can scan all thresholds b and report learning outcomes for all models $h_b \in H$. For non-strategic data, the optimal h^* has $b^* \approx 0$; for strategic data, the optimal h^* can be found using line search. Testing is done on disjoint but similarly sampled held-out features and graph.

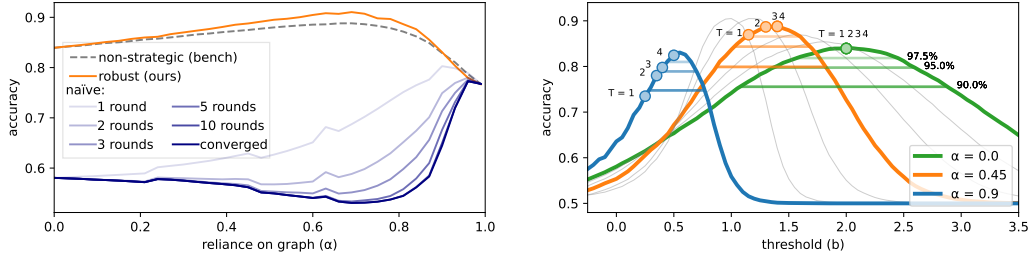


Figure 2: **(Left)** Accuracy of learned \hat{h} for varying graph importances $\alpha \in [0, 1]$. **(Right)** Accuracy for all threshold classifiers h_b , with sensitivity (horizontal lines) and per network depth T (dots).

	Cora	CiteSeer	PubMed
Naïve	52.56 ± 0.20	61.06 ± 0.10	19.02 ± 0.01
Robust (ours)	77.51 ± 0.38	75.21 ± 0.25	82.41 ± 0.38
Non-strategic (benchmark)	87.95 ± 0.08	77.11 ± 0.05	91.34 ± 0.03

Table 1: Test accuracy of different methods. For all results $T = 3$ and $d = 0.25$.

The effects of strategic behavior. Figure 2 (left) presents the accuracy of the learned \hat{h} for varying α and in different settings. In a non-strategic setting (dashed gray), increasing α helps, but if reliance on the graph becomes exaggerated, performance deteriorates ($\alpha \approx 0.7$ is optimal). Allowing users to respond strategically reverses this result: for $\alpha = 0$ (i.e., no graph), responses lower accuracy by ≈ 0.26 points; but as α is increased, the gap *grows*, this becoming more pronounced as test-time response rounds progress (blue lines). Interestingly, performance under strategic behavior is *worst* around the previously-optimal $\alpha \approx 0.75$. This shows how learning in a strategic environment—but *neglecting* to account for strategic behavior—can be detrimental. By accounting for user behavior, our approach (orange line) not only recovers performance, but slightly improves upon the non-strategic setting (this can occur when positive points are properly incentivized; see Appendix D.1).

Sensitivity analysis. Figure 2 (right) plots the accuracy of all threshold models h_b for increasing values of α . For each α , performance exhibits a ‘bell-curve’ shape, with its peak at the optimal h^* . As α increases, bell-curves change in two ways. First, their centers *shift*, decreasing from positive values towards zero (which is optimal for non-strategic data); since using the graph limits users’ effective radius of movement, the optimal decision boundary can be less ‘stringent’. Second, and interestingly, bell-curves become *narrower*. We interpret this as a measure of *tolerance*: the wider the curve, the lower the loss in accuracy when the learned \hat{h} is close to (but does not equal) h^* . The figure shows for a subset of α -s ‘tolerance bands’: intervals around b^* that include thresholds b for which the accuracy of h_b is at least 90%, 95%, and 97.5% of the optimum (horizontal lines). Results indicate that larger α -s provide *less* tolerance. If variation in \hat{h} can be attributed to the number of examples, this can be interpreted as hinting that larger α -s may entail larger sample complexity.

Number of layers (T). Figure 2 (right) also shows for each bell-curve the accuracy achieved by learned models \hat{h} of increasing depths, $T = 1, \dots, 4$ (colored dots). For $\alpha = 0$ (no graph), there are no inter-user dependencies, and dynamics converge after one round. Hence, $T = 1$ suffices and is optimal, and additional layers are redundant. However, as α increases, more users move in later rounds, and learning with insufficiently large T results in deteriorated performance. This becomes especially distinct for large α : e.g., for $\alpha = 0.9$, performance drops by $\sim 11\%$ when using $T = 1$ instead of the optimal $T = 4$. Interestingly, lower T always result in lower, more ‘lenient’ thresholds; as a result, performance deteriorates, and more quickly for larger, more sensitive α . Thus, the relations between α and T suggest that greater reliance on the graph requires more depth.

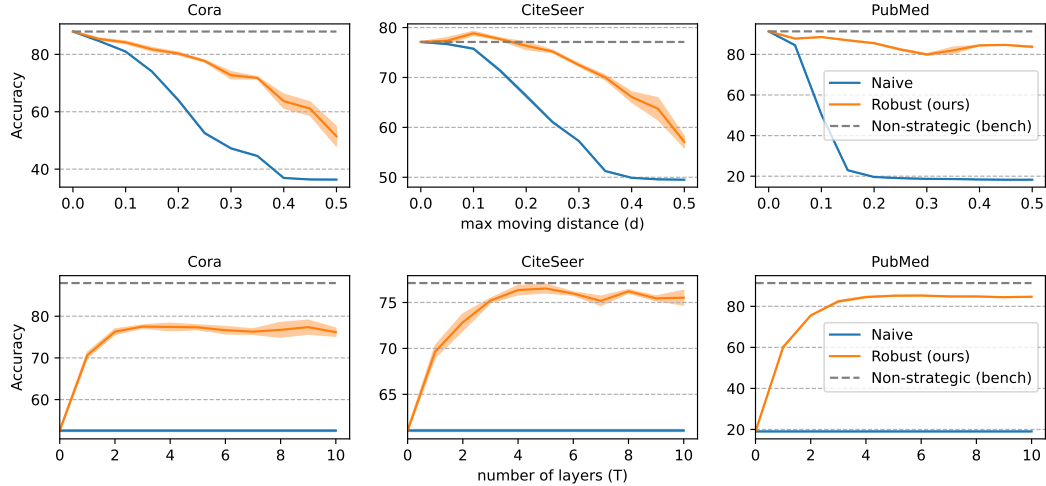


Figure 3: Accuracy for increasing: **(Top:)** max distance d ($T = 3$); **(Bottom:)** depth T ($d = 0.25$).

5.2 EXPERIMENTS ON REAL DATA

Data. We use three benchmark datasets used extensively in the GNN literature: Cora, CiteSeer, and PubMed (Sen et al., 2008; Kipf & Welling, 2017), and adapt them to our setting. We use the standard (transductive) train-test split of Sen et al. (2008); the data is made inductive by removing all test-set nodes that can be influenced by train-set nodes (Hamilton et al., 2017). All three datasets describe citation networks, with papers as nodes and citations as edges. Although these are directed relations by nature, the available data include only undirected edges; hence, we direct edges towards lower-degree nodes, so that movement of higher-degree nodes is more influential. As our setup requires binary labels, we follow standard practice and merge classes, aiming for balanced binary classes that sustain strategic movement. Further details in Appendix C.

Methods. We compare our robust learning approach to a naïve approach that does not account for strategic behavior (i.e., falsely assumes that users do not move). As a benchmark we report the performance of the naïve model on non-strategic data (for which it is appropriate). All methods are based on the SGC architecture (Wu et al., 2019) as it is expressive enough to effectively utilize the graph, but simple enough to permit rational user responses (Eq. (4); see also notes Sec. 1.1). We use the standard weighing scheme of $\tilde{W} = D^{-\frac{1}{2}} A D^{-\frac{1}{2}}$ where A is the adjacency matrix and D is the diagonal degree matrix. Appendix D.2 includes additional results.

Optimization and setup. We train using Adam and set hyperparameters according to Wu et al. (2019) (learning rate=0.2, weight decay= $1.3 \cdot 10^{-5}$). Training is stopped after 20 epochs (this usually suffices for convergence). Hyperparameters were determined based only on the train set: $\tau = 0.05$, chosen to be the smallest value which retained stable training, and $T = 3$, as training typically saturates then (we also explore varying depths). We use β -scaled 2-norm costs, $c_\beta(x, x') = \beta \|x - x'\|_2$, $\beta \in \mathbb{R}_+$, which induce a maximal moving distance of $d_\beta = 2/\beta$. We observed that values around $d = 0.5$ permit almost arbitrary movement; we therefore experiment in the range $d \in [0, 0.5]$, but focus primarily on the mid-point $d = 0.25$ (note $d = 0$ implies no movement). Mean and standard errors are reported over five random initializations. Appendix C includes further details.

Results. Table 1 presents detailed results for $d = 0.25$ and $T = 3$. As can be seen, the naive approach is highly vulnerable to strategic behavior. In contrast, by anticipating how users collectively respond, our robust approach is able to recover most of the drop in accuracy (i.e., from ‘benchmark’ to ‘naïve’; Cora: 35%, CiteSeer: 16%, PubMed: 72%). Note this is achieved with a T much smaller than necessary for response dynamics to converge (T_{\max} : Cora=7, CiteSeer=7, PubMed=11).

Fig. 3 (top) shows results for varying max distances $d \in [0, 0.5]$ and fixing $T = 3$ (note $d = 0$ entails no movement). For Cora and CiteSeer, larger max distances—the result of lower modification

costs—hurt performance; nonetheless, our robust approach maintains a fairly stable recovery rate over all values of d . For PubMed, our approach retains $\approx 92\%$ of the *optimum*, showing resilience to reduced costs. Interestingly, for CiteSeer, in the range $d \in [0.05, 0.15]$, our approach *improves* over the baseline, suggesting it utilizes strategic movements for improved accuracy (as in Sec. 5.1).

Fig. 3 (bottom) shows results for varying depths $T \in \{0, \dots, 10\}$. For all datasets, results improve as T increases, but saturate quickly at $T \approx 3$; this suggests a form of robustness of our approach to overshooting in choosing T (which due to smoothing can cause larger deviations from the true dynamics). Using $T = 1$ recovers between 65%–91% (across datasets) of the optimal accuracy. This shows that while considering only one round of user responses (in which there are no dependencies) is helpful, it is much more effective to consider multiple, dependent rounds—even if only a few.

6 DISCUSSION

In this paper we study strategic classification under graph neural networks. Relying on a graph for prediction introduces dependencies in user responses, which can result in complex correlated behavior. The incentives of the system and its users are not aligned, but also not discordant; our proposed learning approach utilizes this degree of freedom to learn strategically-robust classifiers. Strategic classification assumes rational user behavior; this necessitates classifiers that are simple enough to permit tractable best-responses. A natural future direction is to consider more elaborate predictive architectures coupled with appropriate boundedly-rational user models, in hopes of shedding further light on questions regarding the benefits and risks of transparency and model explainability.

ETHICS AND SOCIETAL IMPLICATIONS

In our current era, machine learning is routinely used to make predictions about humans. These, in turn, are often used to inform—or even determine—consequential decisions. That humans can (and do) respond to decision rules is a factual reality, and is a topic of continual interest in fields such as economics (e.g., Nielsen et al., 2010) and policy-making (e.g., Camacho & Conover, 2013); the novelty of strategic classification is that it studies decision rules that are a product of learned predictive models. Strategic classification not only acknowledges this reality, but also proposes tools for learning in ways that account for it. But in modeling and anticipating how users respond, and by adjusting learning to accommodate for their effects—learning also serves to ‘steer’ its population of users, perhaps inadvertently, towards certain outcomes (Hardt et al., 2022).

GNNs are no exception to this reality. In the domain of graph-based learning, the role of predictive models is expressed in how they associate social connections with decision outcomes for individuals; Clearly, the choice of whether to make use of social data for decisions can be highly sensitive, and doing so necessitates much forethought and care. But the question of whether to use social data to enhance prediction is not a binary in nature, i.e., there is no simple ‘right’ or ‘wrong’. Consider our example of the credit scoring company, Lenddo. On the one hand, Lenddo has been criticized that it may be discriminating applicants based on who they chose to socialize with (or, rather, who chooses to socialize with them). But on the other hand, Lenddo, who focuses primarily on developing countries, has been acclaimed for providing financial assistance to a large community of deserving applicants who, due to conservative norms in typically credit scoring rules, would otherwise be denied a consequential loan.⁹

Such considerations apply broadly. In other focal domains in strategic classification, such as loans, university admissions, and job hiring, the use of social data for informing decision can be highly controversial, on both ethical and legal grounds. Regulation is necessary, but as in similar areas, often lags far behind the technology itself. This highlights the need for transparency and accountability in how, when, and to what purpose, social data is used (Ghalme et al., 2021; Jagadeesan et al., 2021; Bechavod et al., 2022; Barsotti et al., 2022b).

⁹<https://www.motherjones.com/politics/2013/09/lenders-vet-borrowers-social-media-facebook/>

REFERENCES

Saba Ahmadi, Hedyeh Beyhagi, Avrim Blum, and Keziah Naggita. On classification of strategic agents who can both game and improve. *arXiv preprint arXiv:2203.00124*, 2022.

Douglas Almond, Joseph J Doyle Jr, Amanda E Kowalski, and Heidi Williams. Estimating marginal returns to medical care: Evidence from at-risk newborns. *The quarterly journal of economics*, 125(2):591–634, 2010.

Uri Alon and Eran Yahav. On the bottleneck of graph neural networks and its practical implications. In *International Conference on Learning Representations*, 2021. URL <https://openreview.net/forum?id=i80OPhOCVH2>.

Flavia Barsotti, Rüya Gökhan Koçer, and Fernando P Santos. Can algorithms be explained without compromising efficiency? the benefits of detection and imitation in strategic classification. In *Proceedings of the 21st International Conference on Autonomous Agents and Multiagent Systems*, pp. 1536–1538, 2022a.

Flavia Barsotti, Ruya Gokhan Kocer, and Fernando P. Santos. Transparency, detection and imitation in strategic classification. In Lud De Raedt (ed.), *Proceedings of the Thirty-First International Joint Conference on Artificial Intelligence, IJCAI-22*, pp. 67–73. International Joint Conferences on Artificial Intelligence Organization, 7 2022b. doi: 10.24963/ijcai.2022/10. URL <https://doi.org/10.24963/ijcai.2022/10>. Main Track.

Yahav Bechavod, Chara Podimata, Steven Wu, and Juba Ziani. Information discrepancy in strategic learning. In Kamalika Chaudhuri, Stefanie Jegelka, Le Song, Csaba Szepesvari, Gang Niu, and Sivan Sabato (eds.), *Proceedings of the 39th International Conference on Machine Learning*, volume 162 of *Proceedings of Machine Learning Research*, pp. 1691–1715. PMLR, 17–23 Jul 2022.

Aleksandar Bojchevski and Stephan Günnemann. Adversarial attacks on node embeddings via graph poisoning. In *International Conference on Machine Learning*, pp. 695–704, 2019.

Shaked Brody, Uri Alon, and Eran Yahav. How attentive are graph attention networks? In *International Conference on Learning Representations*, 2022. URL <https://openreview.net/forum?id=F72ximsx7C1>.

Michael M. Bronstein, Joan Bruna, Yann LeCun, Arthur Szlam, and Pierre Vandergheynst. Geometric deep learning: Going beyond euclidean data. *IEEE Signal Processing Magazine*, 34(4):18–42, 2017. doi: 10.1109/MSP.2017.2693418.

Michael Brückner and Tobias Scheffer. Nash equilibria of static prediction games. In *Advances in neural information processing systems*, pp. 171–179, 2009.

Michael Brückner and Tobias Scheffer. Stackelberg games for adversarial prediction problems. In *Proceedings of the 17th ACM SIGKDD International Conference on Knowledge Discovery and Data Mining (KDD)*, pp. 547–555, 2011.

Michael Brückner, Christian Kanzow, and Tobias Scheffer. Static prediction games for adversarial learning problems. *The Journal of Machine Learning Research*, 13(1):2617–2654, 2012.

Adriana Camacho and Emily Conover. Manipulation of social program eligibility. *American Economic Journal: Economic Policy*, 3(2):41–65, 2011.

Adriana Camacho and Emily Conover. Effects of subsidized health insurance on newborn health in a developing country. *Economic Development and Cultural Change*, 61(3):633–658, 2013.

Yatong Chen, Jialu Wang, and Yang Liu. Strategic recourse in linear classification. *arXiv preprint arXiv:2011.00355*, 2020.

Andrew Estornell, Sanmay Das, Yang Liu, and Yevgeniy Vorobeychik. Unfairness despite awareness: Group-fair classification with strategic agents. In *Thirty-fifth Conference on Neural Information Processing Systems (NeurIPS), StratML workshop*, 2021.

Ben Finkelshtein, Chaim Baskin, Evgenii Zheltonozhskii, and Uri Alon. Single-node attack for fooling graph neural networks. *arXiv preprint arXiv:2011.03574*, 2020.

Chen Gao, Yu Zheng, Nian Li, Yinfeng Li, Yingrong Qin, Jing Piao, Yuhan Quan, Jianxin Chang, Depeng Jin, Xiangnan He, and Yong Li. Graph neural networks for recommender systems: Challenges, methods, and directions. *ArXiv*, abs/2109.12843, 2021.

Ganesh Ghalme, Vineet Nair, Itay Eilat, Inbal Talgam-Cohen, and Nir Rosenfeld. Strategic classification in the dark. In *Proceedings of the 38th International Conference on Machine Learning (ICML)*, 2021.

Justin Gilmer, Samuel S Schoenholz, Patrick F Riley, Oriol Vinyals, and George E Dahl. Neural message passing for quantum chemistry. In *International conference on machine learning*, pp. 1263–1272. PMLR, 2017.

Ian J. Goodfellow, Jonathon Shlens, and Christian Szegedy. Explaining and harnessing adversarial examples. In Yoshua Bengio and Yann LeCun (eds.), *3rd International Conference on Learning Representations, ICLR 2015, San Diego, CA, USA, May 7-9, 2015, Conference Track Proceedings*, 2015. URL <http://arxiv.org/abs/1412.6572>.

Marco Gori, Gabriele Monfardini, and Franco Scarselli. A new model for learning in graph domains. In *Proceedings. 2005 IEEE International Joint Conference on Neural Networks, 2005.*, 2005.

Michael Großhans, Christoph Sawade, Michael Brückner, and Tobias Scheffer. Bayesian games for adversarial regression problems. In *International Conference on Machine Learning*, pp. 55–63, 2013.

William L. Hamilton, Zhitao Ying, and Jure Leskovec. Inductive representation learning on large graphs. In *NIPS*, 2017.

Moritz Hardt, Nimrod Megiddo, Christos Papadimitriou, and Mary Wootters. Strategic classification. In *Proceedings of the 2016 ACM conference on innovations in theoretical computer science*, pp. 111–122, 2016.

Moritz Hardt, Meena Jagadeesan, and Celestine Mendler-Dünner. Performative power. *arXiv preprint arXiv:2203.17232*, 2022.

Keegan Harris, Hoda Heidari, and Steven Z Wu. Stateful strategic regression. *Advances in Neural Information Processing Systems*, 34:28728–28741, 2021.

Lily Hu, Nicole Immorlica, and Jennifer Wortman Vaughan. The disparate effects of strategic manipulation. In *Proceedings of the Conference on Fairness, Accountability, and Transparency (FAT*)*, pp. 259–268, 2019.

Meena Jagadeesan, Celestine Mendler-Dünner, and Moritz Hardt. Alternative microfoundations for strategic classification. In *International Conference on Machine Learning*, pp. 4687–4697. PMLR, 2021.

Thomas N. Kipf and Max Welling. Semi-supervised classification with graph convolutional networks. In *International Conference on Learning Representations (ICLR)*, 2017.

Tosca Lechner and Ruth Urner. Learning losses for strategic classification. In *Thirty-fifth Conference on Neural Information Processing Systems (NeurIPS), Workshop on Learning in Presence of Strategic Behavior*, 2021.

David S Lee and Thomas Lemieux. Regression discontinuity designs in economics. *Journal of economic literature*, 48(2):281–355, 2010.

Sagi Levanon and Nir Rosenfeld. Strategic classification made practical. In *Proceedings of the 38th International Conference on Machine Learning (ICML)*, 2021.

Sagi Levanon and Nir Rosenfeld. Generalized strategic classification and the case of aligned incentives. In *Proceedings of the 39th International Conference on Machine Learning (ICML)*, 2022.

Jintang Li, Tao Xie, Chen Liang, Fenfang Xie, Xiangnan He, and Zibin Zheng. Adversarial attack on large scale graph. *IEEE Transactions on Knowledge and Data Engineering*, 2021.

Qimai Li, Zhichao Han, and Xiao-Ming Wu. Deeper insights into graph convolutional networks for semi-supervised learning. *Proceedings of the AAAI Conference on Artificial Intelligence*, 32(1), Apr. 2018. URL <https://ojs.aaai.org/index.php/AAAI/article/view/11604>.

Yujia Li, Daniel Tarlow, Marc Brockschmidt, and Richard S. Zemel. Gated graph sequence neural networks. In Yoshua Bengio and Yann LeCun (eds.), *4th International Conference on Learning Representations, ICLR 2016, San Juan, Puerto Rico, May 2-4, 2016, Conference Track Proceedings*, 2016. URL <http://arxiv.org/abs/1511.05493>.

Lydia T Liu, Nikhil Garg, and Christian Borgs. Strategic ranking. In *International Conference on Artificial Intelligence and Statistics*, pp. 2489–2518. PMLR, 2022.

Chinmay Maheshwari, Chih-Yuan Chiu, Eric Mazumdar, Shankar Sastry, and Lillian Ratliff. Zeroth-order methods for convex-concave min-max problems: Applications to decision-dependent risk minimization. In *International Conference on Artificial Intelligence and Statistics*, pp. 6702–6734. PMLR, 2022.

Justin McCrary. Manipulation of the running variable in the regression discontinuity design: A density test. *Journal of econometrics*, 142(2):698–714, 2008.

John P Miller, Juan C Perdomo, and Tijana Zrnic. Outside the echo chamber: Optimizing the performative risk. In *International Conference on Machine Learning*, pp. 7710–7720. PMLR, 2021.

Smitha Milli, John Miller, Anca D. Dragan, and Moritz Hardt. The social cost of strategic classification. In *Proceedings of the Conference on Fairness, Accountability, and Transparency (FAT*)*, pp. 230–239, 2019.

Federico Monti, Davide Boscaini, Jonathan Masci, Emanuele Rodola, Jan Svoboda, and Michael M. Bronstein. Geometric deep learning on graphs and manifolds using mixture model cnns. In *Proceedings of the IEEE Conference on Computer Vision and Pattern Recognition (CVPR)*, July 2017.

Helena Skyt Nielsen, Torben Sørensen, and Christopher Taber. Estimating the effect of student aid on college enrollment: Evidence from a government grant policy reform. *American Economic Journal: Economic Policy*, 2(2):185–215, 2010.

Franco Scarselli, Marco Gori, Ah Chung Tsoi, Markus Hagenbuchner, and Gabriele Monfardini. The graph neural network model. *IEEE transactions on neural networks*, 20(1):61–80, 2008.

Prithviraj Sen, Galileo Namata, Mustafa Bilgic, Lise Getoor, Brian Galligher, and Tina Eliassi-Rad. Collective classification in network data. *AI Magazine*, 29(3):93, Sep. 2008.

Ravi Sundaram, Anil Vullikanti, Haifeng Xu, and Fan Yao. PAC-learning for strategic classification. In *International Conference on Machine Learning*, pp. 9978–9988. PMLR, 2021.

Christian Szegedy, Wojciech Zaremba, Ilya Sutskever, Joan Bruna, Dumitru Erhan, Ian J. Goodfellow, and Rob Fergus. Intriguing properties of neural networks. In Yoshua Bengio and Yann LeCun (eds.), *2nd International Conference on Learning Representations, ICLR 2014, Banff, AB, Canada, April 14-16, 2014, Conference Track Proceedings*, 2014. URL <http://arxiv.org/abs/1312.6199>.

Petar Veličković, Guillem Cucurull, Arantxa Casanova, Adriana Romero, Pietro Liò, and Yoshua Bengio. Graph attention networks. In *International Conference on Learning Representations*, 2018. URL <https://openreview.net/forum?id=rJXMpikCZ>.

Yue Wang, Yongbin Sun, Ziwei Liu, Sanjay E. Sarma, Michael M. Bronstein, and Justin M. Solomon. Dynamic graph cnn for learning on point clouds. *ACM Trans. Graph.*, 38(5), oct 2019. ISSN 0730-0301. doi: 10.1145/3326362. URL <https://doi.org/10.1145/3326362>.

Yanhao Wei, Pinar Yildirim, Christophe Van den Bulte, and Chrysanthos Dellarocas. Credit scoring with social network data. *Marketing Science*, 35(2):234–258, 2016.

Felix Wu, Amauri Souza, Tianyi Zhang, Christopher Fifty, Tao Yu, and Kilian Weinberger. Simplifying graph convolutional networks. In *International conference on machine learning*, pp. 6861–6871. PMLR, 2019.

Zonghan Wu, Shirui Pan, Fengwen Chen, Guodong Long, Chengqi Zhang, and S Yu Philip. A comprehensive survey on graph neural networks. *IEEE transactions on neural networks and learning systems*, 32(1):4–24, 2020.

Keyulu Xu, Weihua Hu, Jure Leskovec, and Stefanie Jegelka. How powerful are graph neural networks? In *International Conference on Learning Representations*, 2019. URL <https://openreview.net/forum?id=ryGs6iA5Km>.

Xiao Zang, Yi Xie, Jie Chen, and Bo Yuan. Graph universal adversarial attacks: A few bad actors ruin graph learning models. In Zhi-Hua Zhou (ed.), *Proceedings of the Thirtieth International Joint Conference on Artificial Intelligence, IJCAI-21*, pp. 3328–3334. International Joint Conferences on Artificial Intelligence Organization, 8 2021.

Hanrui Zhang and Vincent Conitzer. Incentive-aware PAC learning. In *Proceedings of the AAAI Conference on Artificial Intelligence*, 2021.

Xiang Zhang and Marinka Zitnik. Gnnguard: Defending graph neural networks against adversarial attacks. *Advances in Neural Information Processing Systems*, 33:9263–9275, 2020.

Jie Zhou, Ganqu Cui, Shengding Hu, Zhengyan Zhang, Cheng Yang, Zhiyuan Liu, Lifeng Wang, Changcheng Li, and Maosong Sun. Graph neural networks: A review of methods and applications. *AI Open*, 1:57–81, 2020.

Tijana Zrnic, Eric Mazumdar, Shankar Sastry, and Michael Jordan. Who leads and who follows in strategic classification? *Advances in Neural Information Processing Systems*, 34, 2021.

Daniel Zügner and Stephan Günnemann. Adversarial attacks on graph neural networks via meta learning. In *International Conference on Learning Representations*, 2019.

Daniel Zügner, Amir Akbarnejad, and Stephan Günnemann. Adversarial attacks on neural networks for graph data. In *Proceedings of the 24th ACM SIGKDD International Conference on Knowledge Discovery & Data Mining*, 2018.

A ANALYSIS

A.1 HITCHHIKING

Here we provide a concrete example of hitchhiking, following Fig. 1 (E). The example includes three nodes, i, j, k , positioned at:

$$x_k = -3, \quad x_i = -2.1 \quad x_j = -0.5,$$

and connected via edges $k \rightarrow j$, and $j \rightarrow i$. Edge weights $\tilde{w}_{ji} = 0.6$ and $\tilde{w}_{ii} = 0.4$; $\tilde{w}_{kj} = 1/3$ and $\tilde{w}_{jj} = 2/3$; and $\tilde{w}_{kk} = 1$. The example considers a threshold classifier h_b with $b = 0$, and unit-scale costs (i.e., $\beta = 1$) inducing a maximal moving distance of $d = 2$.

We show that i cannot invest effort to cross and obtain $\hat{y}_i = 1$; but once j moves (to obtain $\hat{y}_j = 1$), this results in i also being classified positively (*without* moving). Initially (at round $t = 0$), node embeddings are:

$$\phi_k = -3, \quad \phi_i = -1.14, \quad \phi_j = -\frac{4}{3}$$

and all points are classified negatively, $\hat{y}_k = \hat{y}_i = \hat{y}_j = -1$. Notice that i cannot cross the decision boundary even if she moves the maximal cost-feasible distance of $d = 2$:

$$\phi(x_i^{(0)} + 2; x_{i-}^{(0)}) = \tilde{w}_{ii}(x_i^{(0)} + 2) + \tilde{w}_{ji}x_j^{(0)} = 0.4(-2.1 + 2) + 0.6(-\frac{1}{2}) = -0.34 < 0$$

Hence, i doesn't move, so $x_i^{(1)} = x_i^{(0)}$. Similarly, k cannot cross, so $x_k^{(1)} = x_k^{(0)}$. However, j *can* cross by moving to 1.5 (at cost 2) in order to get $\hat{y}_j = 1$:

$$\begin{aligned} x_j^{(1)} &= 1.5 = -1/2 + 2 = x_j^{(0)} + 2 \\ \Rightarrow \phi(x_j^{(1)}; x_{j-}^{(1)}) &= \tilde{w}_{jj}x_j^{(1)} + \tilde{w}_{kj}x_k^{(0)} = \frac{2}{3}x_j^{(1)} + \frac{1}{3}(-3) = 0 \Rightarrow \hat{y}_j^{(1)} = 1 \end{aligned}$$

After j moves, i is classified positively (and so does not need to move):

$$\phi(x_i^{(1)}; x_{i-}^{(1)}) = \tilde{w}_{ii}x_i^{(1)} + \tilde{w}_{ji}x_j^{(1)} = 0.4(-2.1) + 0.6\frac{3}{2} = 0.06 > 0 \Rightarrow \hat{y}_i^{(2)} = 1$$

A.2 CASCADING BEHAVIOR

We give a constructive example (for any n) which will be used to prove Propositions 3 and 4. The construction is modular, meaning that we build a small ‘cyclic’ structure of size 3, such that for any given n , we simply replicate this structure roughly $n/3$ times, and include two additional ‘start’ and ‘finish’ nodes. Our example assumes a threshold classifier h_b with $b = 0$, and scale costs c_β with $\beta = 1.5$ inducing a maximum moving distance of $d_\beta = 3$.

Let n . We construct a graph of size $n + 2$ as follows. Nodes are indexed $0, \dots, n + 1$. The graph has bi-directional edges between each pair of consecutive nodes, namely $(i, i + 1)$ and $(i + 1, i)$ for all $i = 0, \dots, n$, except for the last node, which has only an outgoing edge $(n + 1, n)$, but no incoming edge. We set uniform normalized edge weights, i.e., $w_{ij} = 1/3$ and $w_{ii} = 1/3$ for all $1 \leq i, j \leq n$, and $w_{0,0} = w_{0,1} = 1/2$ and $w_{n+1,n+1} = w_{n+1,n} = 1/2$. The initial features of each node are defined as:

$$x_0 = -1, \quad x_i = \begin{cases} 2 & \text{if } i \bmod 3 = 1 \\ -4 & \text{o.w.} \end{cases} \quad \forall i = 1, \dots, n + 1 \quad (11)$$

Figure 4 (A) illustrates this for $n = 3$. Note that while the graph creates a ‘chain’ structure, the positioning of node features is cyclic (starting from $n = 1$): 2, -4, -4, 2, -4, -4, 2, ... etc.

We begin with a lemma showing that in our construction, each node $i = 1, \dots, n$ moves precisely at round $t = i$.

Lemma 1. *At every round $1 \leq t \leq n$:*

- (1) *node $i = t$ moves, with $x_i^{(t)} = 5$ if $k \bmod 3 = 1$, and $x_i^{(t)} = -1$ otherwise*
- (2) *all nodes $j > t$ do not move, i.e., $x_j^{(t)} = x_j^{(t-1)}$*

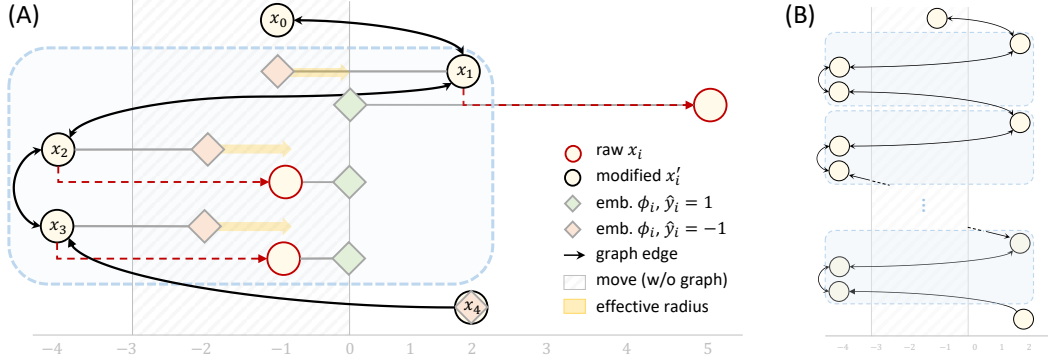


Figure 4: **Cascading behavior.** The construction for Propositions 3 and 4, for: (A) $n = 3$, which includes one copy of the main 3-node module (light blue box), and (B) for any $n > 3$, by replicating the module in sequence (note $|V| = n + 2$).

Note that (1) (together with Prop. 1) implies that for any round t , all nodes $i < t$ (which have already moved at the earlier round $t' = i$) do not move again. Additionally, (2) implies that all $j > t$ remain in their initial position, i.e., $x_j^{(t)} = x_j^{(0)}$. Finally, notice that the starting node x_0 has $\phi_0 = 0.5$, meaning that $\hat{y}_0^{(0)} = 1$, and so does not move at any round.

Proof. We begin with the case for $n = 3$.

- **Round 1:** Node $i = 1$ can cross by moving the maximal distance of 3:

$$\tilde{w}_{1,1}(x_1^{(0)} + 3) + \tilde{w}_{0,1}x_0^{(0)} + \tilde{w}_{2,1}x_2^{(0)} = \frac{1}{3}(2 + 3) + \frac{1}{3}(-1) + \frac{1}{3}(-4) = 0 \quad (12)$$

However, nodes 2,3 cannot cross even if they move the maximal feasible distance:

$$\tilde{w}_{2,2}(x_2^{(0)} + 3) + \tilde{w}_{1,2}x_1^{(0)} + \tilde{w}_{3,2}x_3^{(0)} = \frac{1}{3}(-4 + 3) + \frac{1}{3}(2) + \frac{1}{3}(-4) = -1 < 0 \quad (13)$$

$$\tilde{w}_{3,3}(x_3^{(0)} + 3) + \tilde{w}_{2,3}x_2^{(0)} + \tilde{w}_{4,3}x_4^{(0)} = \frac{1}{3}(-4 + 3) + \frac{1}{3}(-4) + \frac{1}{3}(2) = -1 < 0 \quad (14)$$

- **Round 2:** Node $i = 2$ can cross by moving the maximal distance of 3:

$$\tilde{w}_{2,2}(x_2^{(1)} + 3) + \tilde{w}_{1,2}x_1^{(1)} + \tilde{w}_{3,2}x_3^{(1)} = \frac{1}{3}(-4 + 3) + \frac{1}{3}(5) + \frac{1}{3}(-4) = 0 \quad (15)$$

However, node 3 cannot cross even if it moves the maximal feasible distance:

$$\tilde{w}_{3,3}(x_3^{(1)} + 3) + \tilde{w}_{2,3}x_2^{(1)} + \tilde{w}_{4,3}x_4^{(1)} = \frac{1}{3}(-4 + 3) + \frac{1}{3}(-4) + \frac{1}{3}(2) = -1 < 0 \quad (16)$$

- **Round 3:** Node $i = 3$ can cross by moving the maximal distance of 3:

$$\tilde{w}_{3,3}(x_3^{(2)} + 3) + \tilde{w}_{2,3}x_2^{(2)} + \tilde{w}_{4,3}x_4^{(2)} = \frac{1}{3}(-4 + 3) + \frac{1}{3}(-1) + \frac{1}{3}(2) = 0 \quad (17)$$

Fig. 4 (A) illustrates this procedure for $n = 3$.

Next, consider $n > 3$. Due to the cyclical nature of feature positioning and the chain structure of our graph, we can consider what happens when we sequentially add nodes to the graph. By induction, we can show that:

- $n \bmod 3 = 1$: Consider round $t = n$. Node n has $x_n^{(t-1)} = 2$, and two neighbors: $n - 1$, who after moving at the previous round has $x_{n-1}^{(t-1)} = -1$; and $n + 1$, who has a fixed $x_{n+1}^{(t-1)} = -4$. Thus, it is in the same configuration as node $i = 1$, and so its movement follows Eq. (12).

- $n \bmod 3 = 2$: Consider round $t = n$. Node n has $x_n^{(t-1)} = -4$, and two neighbors: $n-1$, who after moving at the previous round has $x_{n-1}^{(t-1)} = 5$; and $n+1$, who has a fixed $x_{n+1}^{(t-1)} = -4$. Thus, it is in the same configuration as node $i = 2$, and so its movement follows Eq. (15).
- $n \bmod 3 = 0$: Consider round $t = n$. Node n has $x_n^{(t-1)} = -4$, and two neighbors: $n-1$, who after moving at the previous round has $x_{n-1}^{(t-1)} = -1$; and $n+1$, who has a fixed $x_{n+1}^{(t-1)} = 2$. Thus, it is in the same configuration as node $i = 2$, and so its movement follows Eq. (17).

Fig. 4 (B) illustrates this idea for $n > 3$.

□

We now proceed to prove the propositions.

Proposition 3: The proposition follows immediately from Lemma 1; the only detail that remains to be shown is that node $n+1$ does not move at all. To see this, note that since it does not have any incoming edges, its embedding depends only on its own features, x_{n+1} . If $n+1 \bmod 3 = 1$, we have $x_{n+1} = 2$, and so $\hat{y}_{n+1} = 1$ without movement. Otherwise, $x_{n+1} = -4$, meaning that it is too far to cross.

Proposition 4: Fix n and $k \leq n$. Consider the same construction presented above for a graph of size $k+2$. Then, add $n-k$ nodes identical nodes: for each $k < j \leq n$, add an edge $k \rightarrow j$, and set $x_j = x_k - 6$. We claim that all such nodes will move exactly at round k . Consider some node $k < j \leq n$. Since x_k moves only at round k (following Lemma 1), j does not move in any of the first $t \leq k$ rounds:

$$\tilde{w}_{j,j}(x_j^{(0)} + 3) + \tilde{w}_{k,j}x_k^{(0)} = \frac{1}{2}(-x_k^{(0)} - 6 + 3) + \frac{1}{2}(x_k^{(0)}) = \frac{1}{2}(-x_k^{(0)} - 3) + \frac{1}{2}(x_k^{(0)}) = -1.5 < 0 \quad (18)$$

At the end of round $t = k$, node k has a value of $x_k^{(0)} + 3$. This enables j to cross by moving the maximal distance of 3:

$$\tilde{w}_{j,j}(x_j^{(k)} + 3) + \tilde{w}_{k,j}x_k^{(k)} = \frac{1}{2}(-x_k^{(0)} - 6 + 3) + \frac{1}{2}(x_k^{(k)}) = \frac{1}{2}(-x_k^{(0)} - 3) + \frac{1}{2}(x_k^{(0)} + 3) = 0 \quad (19)$$

As this applies to all such j , we get that $n-k$ nodes move at round k , which concludes our proof.

B OPTIMIZATION

B.1 PROJECTION

We prove for 2-norm-squared costs. Correctness holds for 2-norm-costs since the argmin is the same (squared over positives is monotone). Calculation of x_i 's best response requires solving the following equation:

$$\begin{aligned} \min_{x'} c(x'_i, x_i) \quad & \text{s.t.} \quad \theta^\top \phi(x_i; x_{-i}) + b = 0 \\ \min_{x'} \|x'_i - x_i\|_2^2 \quad & \text{s.t.} \quad \theta^\top \phi(x_i; x_{-i}) + b = 0 \end{aligned}$$

To solve for x' , we apply the Lagrange method. Define the Lagrangian as follows:

$$L(x'_i, \lambda) = \|x'_i - x_i\|_2^2 + \lambda[\theta^\top \phi(x_i; x_{-i}) + b]$$

Next, to find the minimum of L , derive with respect to x'_i , and compare to 0:

$$\begin{aligned} 2(x'_i - x_i) + \lambda\theta\tilde{w}_{ii} &= 0 \\ x'_i &= x_i - \frac{\lambda\tilde{w}_{ii}}{2}\theta \end{aligned}$$

Plugging x'_i into the constraint gives:

$$\begin{aligned}\theta^\top [\tilde{w}_{ii}(x_i - \frac{\lambda\tilde{w}_{ii}}{2}\theta) + \sum_{j \neq i} \tilde{w}_{ij}x_j] + b &= 0 \\ \theta^\top [\phi(x_i; x_{-i}) - \frac{\lambda\tilde{w}_{ii}^2}{2}\theta] + b &= 0 \\ \theta^\top \phi(x_i; x_{-i}) + b &= \frac{\lambda\tilde{w}_{ii}^2}{2}\|\theta\|_2^2 \\ 2\frac{\theta^\top \phi(x_i; x_{-i}) + b}{\|\theta\|_2^2 \tilde{w}_{ii}^2} &= \lambda\end{aligned}$$

Finally, plugging λ into the expression for x'_i obtains:

$$x'_i = x_i - \frac{\theta^\top \phi(x_i; x_{-i}) + b}{\|\theta\|_2^2 \tilde{w}_{ii}}\theta$$

B.2 GENERALIZED COSTS

Here we provide a formula for computing projections in closed form for generalized quadratic costs:

$$c(x, x') = \frac{1}{2}(x' - x)^\top A(x' - x)$$

for positive-definite A . As before, the same formula holds for generalized 2-norm costs (since the argmin is the same). Begin with:

$$\begin{aligned}\min_{x'} c(x'_i, x_i) \quad \text{s.t.} \quad &\theta^\top \phi(x_i; x_{-i}) + b = 0 \\ \min_{x'} \frac{1}{2}(x'_i - x_i)^\top A(x'_i - x_i) \quad \text{s.t.} \quad &\theta^\top \phi(x_i; x_{-i}) + b = 0\end{aligned}$$

As before, apply the Lagrangian method:

$$\frac{1}{2}(x'_i - x_i)^\top A(x'_i - x_i) + \lambda[\theta^\top \phi(x_i; x_{-i}) + b]$$

Derivation w.r.t. to x'_i :

$$\begin{aligned}\frac{1}{2}[A^\top(x'_i - x_i) + A(x'_i - x_i)] + \lambda\theta\tilde{w}_{ii} &= 0 \\ (A^\top + A)x'_i &= (A^\top + A)x_i - 2\lambda\theta\tilde{w}_{ii}\end{aligned}$$

Since the matrix $(A^\top + A)$ is PD, we can invert to get:

$$x'_i = x_i - 2\lambda(A^\top + A)^{-1}\theta\tilde{w}_{ii}$$

Plugging x'_i in the constraint:

$$\begin{aligned}\theta^\top [\tilde{w}_{ii}(x_i - 2\lambda(A^\top + A)^{-1}\theta\tilde{w}_{ii}) + \sum_{j \neq i} \tilde{w}_{ij}x_j] + b &= 0 \\ \theta^\top [\phi(x_i; x_{-i}) - 2\lambda(A^\top + A)^{-1}\tilde{w}_{ii}^2\theta] + b &= 0 \\ \theta^\top \phi(x_i; x_{-i}) + b &= 2\lambda\theta^\top(A^\top + A)^{-1}\theta\tilde{w}_{ii}^2\end{aligned}$$

Since $(A^\top + A)^{-1}$ is also PD, we get $\theta^\top(A^\top + A)^{-1}\theta > 0$, and hence:

$$\frac{\theta^\top \phi(x_i; x_{-i}) + b}{2\theta^\top(A^\top + A)^{-1}\theta\tilde{w}_{ii}^2} = \lambda$$

Finally, plugging in λ :

$$\begin{aligned}x'_i &= x_i - \frac{\theta^\top \phi(x_i; x_{-i}) + b}{\theta^\top(A^\top + A)^{-1}\theta\tilde{w}_{ii}^2}(A^\top + A)^{-1}\theta\tilde{w}_{ii} \\ x'_i &= x_i - \frac{\theta^\top \phi(x_i; x_{-i}) + b}{\theta^\top(A^\top + A)^{-1}\theta\tilde{w}_{ii}^2}(A^\top + A)^{-1}\theta\end{aligned}$$

Setting $A = I$ recovers Eq. (7).

Table 2: Real data – statistics and experimental details

	$ V $	$ E $	ℓ	n_{train}	n_{test}^*	negative classes	positive classes	$\%\{y = 1\}$ (train/test)
Cora	2,708	5,728	1,433	640	577	0,2,3	1,4,5,6	44% / 36%
CiteSeer	3,327	4,552	3,703	620	721	0,2,3	1,4,5	50% / 49%
Pubmed	19,717	44,324	500	560	941	1,2	0	21% / 18%

B.3 IMPROVING NUMERICAL STABILITY BY ADDING A TOLERANCE TERM

Theoretically, strategic responses move points precisely on the decision boundary. For numerical stability in classifying (e.g., at test time), we add a small tolerance term, tol , that ensures that points are projected to lie strictly within the positive halfspace. Tolerance is added as follows:

$$\min_{x'} c(x'_i, x_i) \quad \text{s.t.} \quad \theta^\top \phi(x_i; x_{-i}) + b \geq \text{tol} \quad (20)$$

This necessitates the following adjustment to Eq. (7):

$$\text{proj}_h(x_i; x_{-i}) = x_i - \frac{\theta^\top \phi(x_i; x_{-i}) + b - \text{tol}}{\|\theta\|_2^2 \tilde{w}_{ii}} \theta \quad (21)$$

However, blindly applying the above to Eq. (8) via:

$$\text{proj}_h^+(x_i; x_{-i}) = x_i - \min \left\{ 0, \frac{\theta^\top \phi(x_i; x_{-i}) + b - \text{tol}}{\|\theta\|_2^2 \tilde{w}_{ii}} \right\} \theta \quad (22)$$

is erroneous, since any user whose score is lower than tol will move—although in principal she shouldn’t. To correct for this, we adjust Eq. (8) by adding a mask that ensures that only points in the negative halfspace are projected:

$$\text{proj}_h(x_i; x_{-i}) = x_i - \mathbb{1}\{\theta^\top \phi(x_i; x_{-i}) + b < 0\} \cdot \left(\frac{\theta^\top \phi(x_i; x_{-i}) + b - \text{tol}}{\|\theta\|_2^2 \tilde{w}_{ii}} \theta \right) \quad (23)$$

C ADDITIONAL EXPERIMENTAL DETAILS

Data. We experiment with three citation network datasets: Cora, CiteSeer, and Pubmed [Sen et al. \(2008\)](#). Table 2 provides summary statistics of the datasets, as well as experimental details.

Splits. All three datasets include a standard train-validation-test split, which we adopt for our use.¹⁰ For our purposes, we use make no distinction between ‘train’ and ‘validation’, and use both sets for training purposes. To ensure the data is appropriate for the inductive setting, we remove from the test set all nodes which can be influenced by train-set nodes—this ranges from 6%-43% of the test set, depending on dataset (and possibly setting; see Sec. D.2.1). In Table 2, the number of train samples is denoted n_{train} , and the number of inductive test samples is denoted n_{test}^* (all original transductive test sets include 1,000 samples).

Binarization. To make the data binary (original labels are multiclass), we enumerated over possible partitions of classes into ‘negative’ and ‘positive’, and chose the most balanced partition. Experimenting with other but similarly-balanced partitions resulted in similar performance (albeit at times less distinct strategic movement). The exception to this was PubMed (having only three classes), for which the most balanced partition was neither ‘balanced’ nor stable, and so here we opted for the more stable alternative. Reported partitions and corresponding negative-positive ratios (for train and for test) are given in Table 2.

Strategic responses. At test time, strategic user responses are computed by simulating the response dynamics in Sec. 3.1 until convergence.

¹⁰Note that nodes in these sets do not necessarily account for all nodes in the graph.

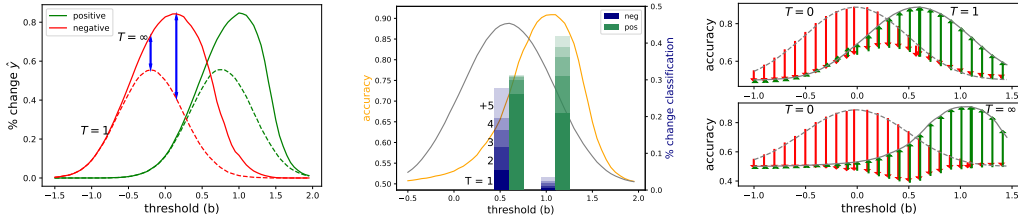


Figure 5: **Synthetic data:** relations between movement and accuracy. All results use $\alpha = 0.7$. **(Left:)** The relative number of points that move for every threshold b , per class, and comparing one round ($T = 1$) to convergence ($T = \infty$). **(Center:)** Accuracy for every threshold b , after one round ($T = 1$) and at convergence ($T = \infty$). For each optimal b , bars show the relative number of points (per class) that obtain $\hat{y} = 1$ due to strategic behavior. **(Right:)** Accuracy for $T = 1$ (top) and $T = \infty$ (bottom), relative to the non-strategic benchmark ($T = 0$), and as a result of strategic movement of negative points (red arrows; decrease accuracy) and positive points (green arrows; improve accuracy).

D ADDITIONAL EXPERIMENTAL RESULTS

D.1 EXPERIMENTS ON SYNTHETIC DATA

In this section we explore further in depth the relation between user movement and classification performance, using our synthetic setup in Sec. 5.1 (all examples discussed herein use $\alpha = 0.7$). From a predictive point of view, graphs are generally helpful if same-class nodes are well-connected. This is indeed the case in our construction (as can be seen by the performance of the benchmark method with non-extreme $\alpha > 0$ values). From a strategic perspective, however, connectivity increases cooperation, since neighboring nodes can positively influence each other over time. In our construction, cooperation occurs mostly within classes, i.e., negative points that move encourage other negative points to move, and similarly for positive points.

Movement trends. Fig. 5 (left) shows how different threshold classifiers h_b induce different degrees of movements. The plot shows the relative number of points (in percentage points) whose predictions changed as a result of strategic behavior, per class (red: $y = -1$, green: $y = 1$) and over time: after one round ($T = 1$, dashed lines), and at convergence ($T = \infty$, solid lines). As can be seen, there is a general trend: when b is small, mostly negative points move, but as b increases, positive points move instead. The interesting point to observe is the gap between the first round ($T = 1$) and final round ($T = \infty$). For negative points, movement at $T = 1$ peaks at $b_1 \approx -0.25$, but triggers relatively little consequent moves. In contrast, the peak for $T = \infty$ occurs at a larger $b_\infty \approx 0.15$. For this threshold, though *less* points move in the first round, these trigger significantly *more* additional moves at later rounds—a result of the connectivity structure within the negative cluster of nodes (blue arrows). A similar effect takes place for positive nodes.

The importance of looking ahead. Fig. 5 (center) plots for a range of thresholds b the accuracy of h_b at convergence ($T = \infty$; orange line), and after one round ($T = 1$; gray line). The role of the latter is to illustrate the outcomes as ‘perceived’ by a myopic predictive model that considers only one round (e.g., includes only one response layer $\tilde{\Delta}$); the differences between the two lines demonstrate the gap between perception (based on which training chooses a classifier \hat{h}) and reality (in which the classifier \hat{h} is evaluated). As can be seen, the myopic approach leads to an under-estimation of the optimal b^* ; at $b_1 \approx 0.5$, performance for $T = 1$ is optimal, but is severely worse under the true $T = \infty$, for which optimal performance is at $b_\infty \approx 1.15$.

The figure also gives insight as to *why* this happens. For both b_1 and b_∞ , the figure shows (in bars) the relative number of points from each class who obtain $\hat{y} = 1$ as a result of strategic moves. Bars are stacked, showing the relative number of points that moved per round T (darker = earlier rounds; lightest = convergence). As can be seen, at b_1 , the myopic models believes that many positive points, but only few negative points, will cross. However, in reality, at convergence, the number of positive points that crossed is only slightly higher than that of negative points. Hence, the reason for the (erroneous) optimism of the myopic model is that it did not correctly account for the magnitude of

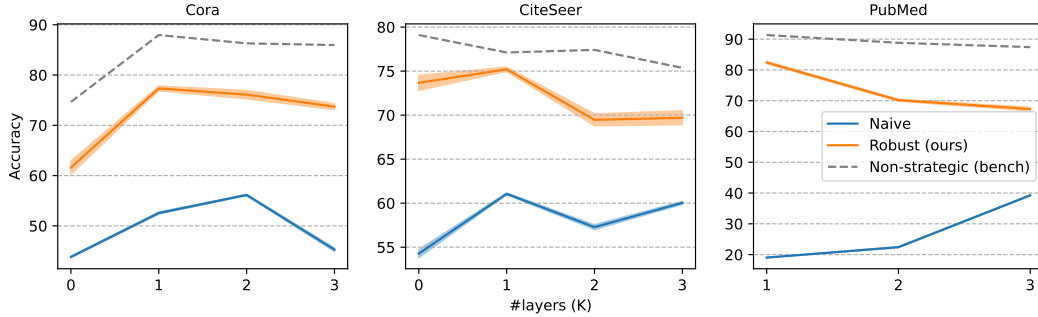


Figure 6: Accuracy for varying number of SGC layers (K). Note test sets may vary across K .

correlated moves of negative points, which is expressed over time. In contrast, note that at b_∞ , barely any negative points cross.

How movement affects accuracy. An important observation about the relation between movement and accuracy is that for any classifier h , any *negative* point that moves *hurts* accuracy (since $y = -1$ but predictions become $\hat{y} = 1$), whereas any *positive* point that moves *helps* accuracy (since $y = 1$ and predictions are now $\hat{y} = 1$). Fig. 5 (right) shows how these movements combine to affect accuracy. The figure compares accuracy before strategic behavior ($T = 0$; dashed line) to after one response round ($T = 1$; solid line, top plot) and to convergence ($T = \infty$; solid line, lower plot). As can be seen, for any b , the difference between pre-strategic and post-strategic accuracy amounts to exactly the degradation due to negative points (red arrows) plus the improvement of positive points (green arrows).

Note, however, the difference between $T = 1$ and $T = \infty$, as they relate to the benchmark model ($T = 0$, i.e., no strategic behavior). For $T = 1$ (top), across the range of b , positive and negative moves roughly balance out. A result of this is that curves for $T = 0$ and $T = 1$ are very much similar, and share similar peaks in terms of accuracy (both have ≈ 0.89). One interpretation of this is that if points were permitted to move only one round, the optimal classifier can completely recover the benchmark accuracy by ensuring that the number of positive points the moves overcomes the number of negative points. However, for $T = \infty$ (bottom), there is a *skew* in favor of positive points (green arrows). The result of this is that for the optimal b , additional rounds allow positive points to move in a way that obtains slightly *higher* accuracy (0.91) compared to the benchmark (0.89). This is one possible mechanism underlying our results on synthetic data in Sec. 5.1, and later for our results on real data in Sec. 5.2.

D.2 EXPERIMENTS ON REAL DATA

D.2.1 EXTENDING NEIGHBORHOOD SIZE

One hyperparameter of SGC is the number ‘propagation’ layers, K , which effectively determines the graph distance at which nodes can influence others (i.e., the ‘neighborhood radius’). Given K , the embedding weights are defined as $\tilde{W} = D^{-\frac{1}{2}} A^K D^{-\frac{1}{2}}$ where A is the adjacency matrix and D is the diagonal degree matrix. For $K = 0$, the graph is unused, which results in a standar linear classifier over node features. Our results in the main body of the paper use $K = 1$.

Fig. 6 shows results for an increasing K (we set $T = 3, d = 0.25$ as in our main results). Results are mixed: for PubMed, higher K seems to lead to less drop in accuracy for naïve and less recovery for our approach; for Cora and CiteSeer, results are unstable. Note however that this may likely be a product of our inductive setup: since varying K also changes the effective test set (since to preserve inductiveness, larger K often necessitates removing more nodes), test sets vary across conditions and decrease in size, making it difficult to directly compare result across different K .

D.2.2 STRATEGIC IMPROVEMENT

Our main results in Sec. 5.2 show that for CiteSeer, our strategically-aware approach outperforms the non-strategic benchmark (similarly to our synthetic experiments). Here we show that these results are robust. Fig. 7 provides higher-resolution results on CiteSeer for max distances $d \in [0, 0.22]$ in hops of 0.01. All other aspects the setup match the original experiment. As can be seen, our approach slightly but consistently improves upon the benchmark until $d \approx 0.17$.

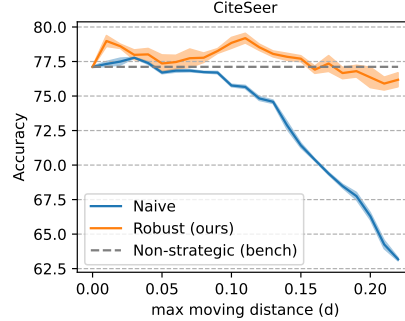


Figure 7: Accuracy on CiteSeer for increasing max distance d (focused and higher-resolution).